HHS Public Access

Author manuscript

Trans Soc Min Metall Explor Inc. Author manuscript; available in PMC 2018 May 17.

Published in final edited form as:

Trans Soc Min Metall Explor Inc. 2017 ; 342(1): 51–61. doi:10.19150/trans.8108.

Methane emissions and airflow patterns on a longwall face: Potential influences from longwall gob permeability distributions on a bleederless longwall panel

S.J. Schatzel,

Research geologist, National Institute for Occupational Safety and Health, Pittsburgh, PA, USA

R.B. Krog, and

Mining engineer, West Virginia University, Morgantown, WV, USA

H. Dougherty

Mining engineer, National Institute for Occupational Safety and Health, Pittsburgh, PA, USA

Abstract

Longwall face ventilation is an important component of the overall coal mine ventilation system. Increased production rates due to higher-capacity mining equipment tend to also increase methane emission rates from the coal face, which must be diluted by the face ventilation. Increases in panel length, with some mines exceeding 6,100 m (20,000 ft), and panel width provide additional challenges to face ventilation designs.

To assess the effectiveness of current face ventilation practices at a study site, a face monitoring study with continuous monitoring of methane concentrations and automated recording of longwall shearer activity was combined with a tracer gas test on a longwall face. The study was conducted at a U.S. longwall mine operating in a thick, bituminous coal seam and using a U-type, bleederless ventilation system. Multiple gob gas ventholes were located near the longwall face. These boreholes had some unusual design concepts, including a system of manifolds to modify borehole vacuum and flow and completion depths close to the horizon of the mined coalbed that enabled direct communication with the mine atmosphere. The mine operator also had the capacity to inject nitrogen into the longwall gob, which occurred during the monitoring study. The results show that emission rates on the longwall face showed a very limited increase in methane concentrations from headgate to tailgate despite the occurrence of methane delays during monitoring.

Average face air velocities were 3.03 m/s (596 fpm) at shield 57 and 2.20 m/s (433 fpm) at shield 165. The time required for the sulfur hexafluoride (SF_6) peak to occur at each monitoring location has been interpreted as being representative of the movement of the tracer slug. The rate of movement of the slug was much slower in reaching the first monitoring location at shield 57 compared with the other face locations. This lower rate of movement, compared with the main face ventilation, is thought to be the product of a flow path within and behind the shields that is moving in the general direction of the headgate to the tailgate. Barometric pressure variations were pronounced over the course of the study and varied on a diurnal basis.

Disclaimer

The findings and conclusions in this report are those of the authors and do not necessarily represent the views of NIOSH.

Keywords

Methane emissions; Longwall ventilation; Permeability distributions

Introduction

Researchers at the Pittsburgh Mining Research Division (PMRD) of the U.S. National Institute for Occupational Safety and Health (NIOSH) conducted a study to determine flow rates and identify pathways of movement for methaneair mixtures in the longwall face and gob of a bleederless longwall operation. One objective of this study was to obtain information from tracer gas tests to better understand the flow of air/methane in the vicinity of the longwall face, through the gob and possibly to operating gob gas ventholes (GGVs), also referred to as gob vent boreholes. The design of the experiment includes a means of sampling unreachable parts of the longwall gob.

An additional objective examined face methane emission rates in the vicinity of the longwall face area. The face emission monitoring task was designed to continuously monitor volumes of methane emitted during longwall mining and to describe its movement on the face and in the vicinity of the tailgate corner. The research study focused on air and methane transport pathways along a longwall face, air and methane flow out of the tailgate, and potential interaction between face air and the front of the gob.

Field studies have the inherent limitation of only testing the mining parameters, geology and mining conditions that exist at the study site. Another parameter of interest was the panel engineering and whether it was designed as subcritical or supercritical, which influences gob caving characteristics and gob gas transport. Ventilation characteristics of western and eastern coal basin geology are generally influenced by the cleat development of the coal and the stratigraphy near the mined horizon. The specific conditions at this mine are discussed later. However, it is important to recognize how these variables have a direct impact on ventilation demands in coal mining.

Managing methane in longwall gobs

Prior research has shown the potential influence of GGV production on longwall face methane concentrations (Mucho et al., 2000). However, these evaluations were performed in the Northern Appalachian Basin, not the geographic basin where this study site is located. In general, the transport network related to GGV performance is produced by mining-induced fractures behind the longwall face. In the United States, key GGV design parameters related to production have been reported (Karacan et al., 2007; Schatzel, Karacan et al., 2012). The operator configured GGVs to be drilled and completed near the mined coal bed, terminating about 15 m (50 ft) into the caved material from the tailgate entry. Borehole completion depths typically terminate above the caving depth for mines operating in the Northern Appalachian Basin, but they extended into the caved zone at the study site, according to generalized values for roof caving heights reported by Singh and Kendorski (1981).

Through research on coalbed methane production and control on longwalls, much has been learned about managing this gas to maintain a safe work environment. In general, the primary gas migration pathways in the gob are paralleling the gateroads on the headgate and tailgate edges or near margin locations (Diamond, Jeran and Trevits, 1994; Schatzel, Karacan et al. 2012). Gas migration along these pathways is favored by the high permeability zones found in the overburden paralleling the gateroads due the collapsed rock in the space formerly occupied by the coalbed bordering the gateroad pillars, which still provide some ability for roof support inby the longwall face (Figs. 1a and 1b). The former gateroads inby the face are in most cases not travelable but the degree of support they provide (and any additional roof support installed by the mine) allows the overburden to "drape," creating tensional stress and enhancing permeability. The overall design of the GGV borehole, especially its depth and completion method, strongly influence the behavior and performance of the GGV. If the bottom of the GGV penetrates the caved zone of the gob, it is likely that some ventilation air will be produced if an exhauster is used at the surface to extract gas. If the completion is further above the mined coal unit, the GGV will intercept the fracture network where permeability will be lower and little or no ventilation air will be extracted. The engineering design of the longwall panel is also a factor in GGV performance. Supercritical longwall panels have a greater width than overburden depth, and a subcritical design has a greater depth than width. These two designs influence the caving characteristics of the fractured gob and thereby the permeability distribution, although both designs produce the pattern of enhanced permeability adjacent to the gateroads.

Study site and mine design

The study was conducted at a western longwall coal mine with bleederless ventilation, GGVs, and nitrogen (N_2) injection. The multiple panel district is acted upon by surface exhaust fans (Fig. 2). In this application, the surface exhaust fans ventilate the tailgate entries adjacent to the active panel and maintain a negative pressure on the seals adjacent to the gob from the prior mined panel (Fig. 2). This mine configuration is more typical of bleederless ventilation system mine designs than U.S. coal mines that use bleeder systems to ventilate pillared worked-out areas, due to the need to minimize oxygen interaction within the worked-out area to reduce the potential for spontaneous combustion to occur.

The mine has one longwall section and uses a three-entry gateroad system (Fig. 2). The mine progressively installs interpanel seals in the headgate crosscuts between entries 2 and 3. Consequently, there is a significant amount of air directed inby the longwall face in headgate entries 1 and 2 in addition to air directed across the face and outby in the headgate belt entry. Gate road entries are numbered from right to left in the orientation shown in the figure. After intake air crosses the face, it is directed outby by a curtain in the tailgate and then continues moving outby in tailgate entries 1 and 2. A line of interpanel seals isolates tailgate entry 3 and the prior mined-out panel from the study panel. The overburden is variable and averaged 180 m (600 ft) in the vicinity of the longwall during the NIOSH field experiments. The overburden contains substantial thicknesses of shale and siliclastic sedimentary units, which influence mechanical failure characteristics during undermining. This appears to produce a tendency to hold up the roof in the vicinity of the face near the front of the gob. The mine operator places GGVs in a near-margin configuration on the tailgate side very near the outer

margin on the coal block, near the zone of maximal rock tension in the overburden (Diamond, Jeran and Trevits, 1994; Schatzel, Krog et al., 2012). The GGVs were placed at close intervals of about 60 m (200 ft), and sometimes less than 30 m (100 ft), between holes (Fig. 3).

The mine operator also reported evidence of a void space, which is a result of caving parallel, above and behind the face. In the most general sense, void space exists behind a longwall face, at the front of the mined-out longwall block, in many longwall coal mines. For example, larger volumes of void spaces reported by mine operators were enhanced by thick coal, over 2.1 m (7 ft) in height; long faces, about 300 m (1,000 ft) or more; very competent strata, frequently siliclastic rock adjacent to the mine workings; and possibly friable coal, which may slough in the vicinity of the face (Schmidt, 2016). All but the last condition were met at the study site.

The mine operator uses an unusual exhauster system on the GGVs to extract gas from the boreholes at the surface. The exhausters use diesel-powered engines instead of combusting the produced gas or using electrically powered motors. Consequently, the exhausters can be operated when no methane is being produced, and a manifold allows the GGVs to completely extract the gas in the borehole in full production mode, operate without producing any coalbed gas and produce gas mixtures in between these two endpoints. The operator also utilizes N_2 injection into the longwall panel gob. This N_2 is pumped underground to maintain an inert atmosphere in the gob. Unfortunately, the mine operator only keeps records on the quantity being pumped underground over time. The distribution of the gas underground among multiple potential outlets is not known. The injection of N_2 into the mined out area of the active panel was used by the operator to inert the methane mixture in the gob and to add gas volume to these areas during periods of increasing barometric pressure, diminishing the effect of the contraction of these gases.

Methodology

Tracer gas testing

The initial research phase for this study consisted of a tracer gas test. Tracer gas was released behind the first two headgate shields, with air samples taken along the longwall face, outby the face in the tailgate, and on the surface at the producing GGVs. The gas release and subsequent monitoring continued for one nonproduction shift. The retrieved air samples were analyzed for tracer gas concentration. Also, a ventilation survey was made by taking measurements at underground monitoring locations to determine airflow distribution around the study panel. Data from the ventilation survey are shown in Table 1 and Fig. 4.

The panel block width for the study panel had a face width of 300 m (1,000 ft). The coalbed mining height was 3.4 m (11 ft), and 176 longwall shields were located on the face. Tubing lines were installed at the longwall face with sampling intakes located at shields 57, 119 and 165, resulting in a spacing between tubing inlets of roughly 90 m (300 ft). Face tubing inlets were positioned at the centerline of the shields immediately under the canopy and over the walkway on the face. An additional near-face monitoring location using tubing was installed approximately 24 m (80 ft) outby the working face in the tailgate gateroad (Fig. 3). The

polyethylene tubing had a 0.953-cm (0.375-in.) inside diameter and 1.3-cm (0.5-in) outside diameter with couplers joining the tubing sections and filters on each inlet. Samples were drawn through the tube bundles using permissible and MSHA-approved SKC Airchek 224-44XRM pumps (SKC Inc., Eighty Four, PA).

Knowing the pump rates and sulfur hexafluoride (SF_6) transit times through the tubing, incremental gas sampling was performed at the sample pump station using Vacutainer resealable glass vials (Becton Dickinson, Franklin Lakes, NJ). Tracer gas volumes were determined using methods previously described by Thimons and Kissell (1974) and Hartman et al. (1997) using a rapid gas release. Surface monitoring at GGVs included those with operating exhausters near the working face on the study panel (Fig. 3). Monitoring included GGVs 1 through 6, with the most frequent monitoring at the four closest holes inby the face, which were GGVs 3 to 6. Barometric pressure was monitored continuously during the field study. The flow of nitrogen being delivered to the active panel headgate was also monitored.

Methane monitoring

Following the completion of tracer gas testing on the study panel, a monitoring study was conducted to measure methane concentrations and gas flows along the face and outby the tailgate corner. Monitoring was conducted during three successive shifts of daytime coal production. Face methane monitoring equipment was installed during the preceding nonproduction period. Industrial Scientific ATX 620 instruments (Industrial Scientific, Pittsburgh, PA) were utilized and set to record one-minute-averaged data, rounded to the nearest tenth of a percent, with data stored on the instrument data logger. These are multigas, portable instruments, and the reported methane data was produced by conventional 0 to 5 percent lower explosive limit, or LEL, technology for combustible gases. Instrument monitoring locations included all of those used for the tracer gas study plus an additional location at the tailgate corner, or five near-face instruments: those at shields 57, 119 and 165, at the tailgate, and at least 24 m (80 ft) outby the longwall face in the tailgate entry (Fig. 3). A second set of monitors was installed in the face area by the operator with methanometers at shields 4, 88 and 176 (the last tailgate shield) and at the 24-m (80-ft) outby location. Mine operator instruments were part of the approved ventilation plan. Tubing inlet locations were over the walkway on the longwall face for the NIOSH instrumentation. The operator instrumentation was set to record instantaneous readings, as allowed by the response time of the methane sensors. Both sets of 24-m (80-ft) sensors were located about 46 m (150 ft) outby the face at the start of each shift. An additional methane monitor installed by the operator was located at the regulator for the return air coming off of the production panel. These data are not included in the plots because they include the face area and mined-out portion of the panel plus emissions from the rib emissions of the unmined panel that are not within the scope of the study.

The sampling strategy for methane monitoring at the GGVs was identical to that used for the tracer gas test, with five borehole sites being sampled and the four near-face boreholes — GGVs 3, 4, 5 and 6 — undergoing the most frequent monitoring (Fig. 3). A portion of the samples collected from the GGVs during the methane monitoring experiment were analyzed

for tracer gas concentrations to address the potential for gas migration from the face to the gob.

Discussion and results

Tracer gas testing

During the tracer gas test, two lecture bottles of 99.95 percent SF_6 were released in succession, totaling 80.7 L (2.85 cu ft) at underground ambient conditions. The release location was positioned about 0.6 m (2 ft) below the roof. The shearer was located at shield 10 for the tracer gas test. The polyvinyl chloride pipe used for the release was about 1.8 m (6 ft) in length. The presence of void space behind the shields was observed during the study, although the void dimensions are not known. Recovery of tracer gas was measured at monitoring location 1 at shield 57, or a distance of about 99.4 m (326 ft) from the start of the headgate shield line. The SF_6 volume recovered at location 1 was 150 L (5.30 cu ft), or roughly 190 percent of the released gas. The primary causes of tracer gas volumetric recovery problems are incomplete mixing of the tracer in the ambient air, the existence of unmonitored flow paths, an undesirable amount of released tracer gas (too much or too little), or instrument/analytical problems related to the release or recovery (Grot and Lagus, 1991; American Society of Testing Materials, 1999, 2000). The primary cause of high errors in this study is thought to be bias in the determination of the highest concentration samples. Tracer gas recovery at the 24 m (80 ft) sensor was measured to be 115 L (4.06 cu ft). The lower recovered volume at this location is likely due to the loss of air carrying SF_6 to unplanned migratory pathways.

The GGVs at the study site were drilled deep enough to penetrate the longwall gob caved zone, which may have allowed for increased connectivity to the void space behind the longwall shields, creating a potential pathway for the movement of tracer gas. Interaction between the face ventilation air and the GGVs was also thought to be possible due to the close proximity of the boreholes to the tailgate, within 15 m (50 ft) of the panel margin where enhanced zones of permeability have been shown to exist. Gobs in U.S. longwall mines can be very expansive in area — for example, 2,000,000 m^2 (22,000,000 ft^2). The conducting of tracer gas studies to include these zones requires sufficient volumes of SF_6 to keep concentrations of the tracer above detection limits. In this study, the SF_6 concentrations measured at nearface locations were initially above optimal concentrations for gas chromatographic analysis (NIOSH, 1994).

Plots of the SF_6 concentration over time for the face and tailgate locations are shown in Fig. 4. The shield 57 location, being the sampling point closest to the release point, was used to determine the amount of SF_6 recovered. Because samples were drawn through tube bundles, a time delay was inherent in the transport of gas through the sampling lines. The time delays for each sample line were calculated, and these delays were subtracted from the arrival times to show the actual times of tracer gas recovery in Fig. 4. A concentration peak is seen at location 2 (shield 119), about four minutes after the release and prior to the peak for location 1 (shield 57). All times are rounded to the nearest minute due to the face air sampling frequency of the Vacutainer bottles. About two minutes later, peaks occur at location 1 (shield 57), with peaks at locations 3 and 4 arriving essentially simultaneously in the same

minute as the SF_6 arrival at location 1 (Fig. 4). The sequence of peaks at locations 1 and 2 in real time is likely the product of multiple migration pathways in front of and behind the shield line from the release point to the shield 57 and 119 tubing inlets.

Most investigations of airflow on longwall faces have assumed that transport occurs in a linear path with air quantities moving from head to tail (Srinivasa et al., 1993; Krog et al., 2006; Schatzel et al., 2006). Airflow velocities determined by multiple methods are shown in Table 1. The velocities shown are a product of measurements in the face area, calculations based on tracer gas arrivals, and calculations based on tracer gas peak accumulations. More specifically, the arrival-based velocities used the time of the beginning of the release to the time of the first show of tracer gas over the gas chromatographic detection limit, and the peak-based velocities were determined from the midpoint time of the release to the time of the concentration peak occurrence and the distance traveled. Field-based measurements were done with a vane anemometer, and cross-sectional areas were measured with a permissible, laser instrument. The air flow velocities based on tracer gas arrivals correlate quite well with the velocities determined from flow measurements made in the face area. These data show a relatively consistent velocity for all four tubing inlet locations. Airflows determined for NIOSH monitoring locations are also shown.

The arrival-based velocities are the tracer gas data most correlative to conventional anemometer measurements (Table 1 and Fig. 4). The peak data in this study are produced by the accumulation of SF_6 slug over multiple minutes and represent the dominant pathway of the tracer gas movement and accumulation.

The data suggest that a small portion of the released gas reached the face airflow to be retrieved at the location 1 tubing inlet, which represents the arrival time at the concentration of about 800 ppb SF_6 in air. It is proposed that the relatively large difference between arrival and peak velocity data at shield 57 is the product of the released SF_6 moving both in the face air at a relatively high velocity — in the range of the arrival time data — and also behind the face in a lower velocity air stream. The movement of tracer gas onto the face appears to have occurred primarily past location 1 as the airflow velocities, based on arrivals, between locations 2 and 3 are similar to the velocities between tubing inlets 3 and 4 (Table 1 and Fig. 4). If the SF_6 transport to location 2 was a combination of airflow in front of and behind the shield line, the determined velocity would have been a lower combination of rates from the two flow regimes. A value about 0.35 m/s (68 ft/min) is shown for location 1 in the peak-based data of Table 1. However, the arrival time data are typically in much closer agreement than the peak accumulation data to the actual flow measurements.

The samples retrieved from the GGVs (Fig. 5) were analyzed for either tracer gas concentration or for full hydrocarbon and gas compositional analysis. The SF_6 monitoring of the GGVs indicated arrivals of this gas in the two producing boreholes closest to the mine face (Fig. 3). Low-concentration arrivals of SF_6 were first noted at GGV 6 at about 47 min after the underground release. After the first appearance of tracer gas at the GGVs very near the detection limit of the gas chromatograph, there were intermittent lapses in the presence of tracer gas in the GGV exhaust. Tracer gas at GGV 5 was measured about 3 h 48 min following the initial release. Average flows from the GGVs are given in Table 2. At this

time, the face location was about 30 m (100 ft) outby GGV 6 during the tracer gas test and 52 m (170 ft) outby GGV 5. Assuming the shortest possible distance for the arrival times to GGV 6, the rate of SF_6 movement to the borehole was about 0.0066 m/s (1.3 ft/min). For GGV 5, the migration rate, assuming a minimum distance, was 0.0036 m/s (0.7 ft/min). Tracer gas was detected at GGV 4 the day after the SF_6 release. Borehole GGV 4 was located about 90 m (300 ft) from the longwall face during the tracer gas test. The arrival of the SF_6 at GGV 4 was detected at 14:15 on day 2 of the study. Using the approximate minimum distance, the transport rate of the tracer gas to GGV 4 was about 0.001 m/s (0.2 ft/min).

Measurements were made of tracer gas migration rates in prior NIOSH research in the fractured overburden above gateroads in the Northern Appalachian Basin (Schatzel et al., 1999; Mucho et al., 2000). These field-based studies were conducted at longwall mines operating in the Pittsburgh coalbed in southwestern Pennsylvania. Transport rates of tracer gas through the mining-induced fracture network that were measured in gobs were of the same order of magnitude as the results from this study. Transport times and permeability in the fractured gob overburden were found to be highly influenced by longwall face proximity and associated subsidence in the Northern Appalachian Basin. The zone of maximum GGV production was determined to be located about 60 m (200 ft) behind the face. The majority of surface subsidence was observed to end in that study about 88 m (290 ft) behind the face (Palchik, 2003; Schatzel, Karacan, et al., 2012). It should be noted that borehole completion designs used at the study mine site and at the Northern Appalachian Basin coal mine differ significantly. Ground movement characteristics are strongly influenced by panel dimensions and overburden depths, which are also dissimilar at the eastern and western U.S. sites. Both the study site and the eastern U.S. sites used supercritical longwall ground control designs.

Methane monitoring

Methane monitoring was planned for field study days 2 through 4. For a portion of the monitoring period, coal production was below the level typical of the mine. Becuase the study panel had a bleederless ventilation configuration, gas liberation into the tailgate entry was inclusive of multiple emission sources. One source of gas reaching the tailgate is from the front of the gob, behind the face airflow that moves in the general direction paralleling the face toward the tailgate corner and tailgate entry. Gas liberated deeper in the gob moves in the general direction of the face because no bleeder pathways exist at the back of the panel for potential gas migration. The gob gas typically moves toward the front of the gob and is eventually carried in the direction of the tailgate and the tailgate entry. Another source of methane reaching the tailgate corner is from the unmined coal face.

Consequently, day 3 of the monitoring data was dropped from subsequent analysis due to low coal production and potential problems in interpreting the emissions monitoring data. Some sensor malfunctions occurred on the NIOSH instrumentation during the monitoring period, which required removal and replacement of the sensor unit between in-mine monitoring periods. Typical of the methane sensor failures was a consistent rise of the sensor data output once failure began. This behavior is apparent in the NIOSH shield 119 sensor data on day 2 of the field study, with erroneous output starting between about 15:00 and

16:48 (Figs. 6a and 6b). No corresponding rise in methane emissions was depicted in the other NIOSH sensors or in the mine operator's instrumentation (Figs. 6a and b). However, other than for the shield 119 instrument, there is considerable agreement between the two instrument arrays and there is a general increase in methane emissions in the airstream indicated as ventilation air moves across the face. Shearer cutting activity, as indicated by the tram speed graph, produced increases in methane, although sumping in of the shearer generally resulted in a smaller emissions increase (Figs. 6a, 6b and 6c). The 24-m (80-ft) sensor for the mine operator data depicted a rise in methane emissions exceeding levels shown from the other sensors and generally exceeding emissions from the NIOSH sensors, except for the previously mentioned shield 119 instrument. Methane flow at the 24-m (80-ft) sensor was significantly above that of the tailgate sensor, on the order of 0.20 m^3/s (420 cfm). As both gas in the gob and air on the face move predominantly toward the tailgate corner in this U-type ventilation design, the highest concentration at the 24-m (80-ft) sensor is not surprising and may differ from ventilation and gas flow patterns on longwalls with effective bleeder systems. The mine completed six passes of the shearer during day 2 emissions monitoring.

Results from emissions monitoring on day 4 are shown in Fig. 7. Despite a longer period of face monitoring on day 4 compared with day 2, only four passes were completed by the longwall shearer. The NIOSH sensors showed small increases in methane emissions as airflow moved toward the tailgate (Fig. 7a). Data from the mine operator's instruments correspond well with the trends in the NIOSH emission curves. The methane emissions curves from the mid-face locations (shields 88 and 119) and the 24-m (80-ft sensor) are very similar for the two datasets (Figs. 7a and 7b). Although the NIOSH instrumentation showed slightly more methane flow, the relative increase in methane flow from the tailgate instrument to the 24-m (80-ft) sensor is similar on the two plots, on the order of 0.20 to about 0.35 m^3/s (420 to 740 cfm) in both arrays. This increase at this location far exceeded the increase in face emissions. Figure 7c shows the shearer tram speed and periods of sumping in on the longwall face. Rapid cutting activity did correspond to increased methane emissions at the sensors, particularly when cutting was not associated with sumping in. Despite the relatively low methane emissions from the longwall face, methane delays did occur during the study. As the face emission rates were relatively low during the monitoring, they did not strongly influence the occurrence of methane delays during the study (Table 3). Compared with other monitoring locations, greater increases in methane concentrations were measured at the 24-m (80-ft) sensor, and methane accumulations at that location were the most frequent source of methane delays. As the only potential contributors to increased emissions at the 24-m (80-ft) sensor were the longwall face and the air entering the tailgate from the worked-out area, the source of increased, problematic methane emissions appeared to be associated with areas where there was inflow from the tailgate and the gob (Fig. 3). Another potential path of gas movement is migration from the gob to the face through the longwall shield legs.

The data shown in Table 3 suggest that the most problematic increases in methane concentrations due to methane emissions on the longwall section are not the result of face-specific emissions. The coal cleat system is not well-developed at this site, which may tend to produce more sporadic, less consistent emission of gas through the cleat fracture network

(Karacan et al., 2007; Karacan, 2008). Relatively low coalbed methane gas content may also be responsible for the limited level of face emissions. The mine site is operating in the No. 8 coal seam, and the overlying No. 9 seam is a possible emissions source and is located within the zone of emissions. The rank of both seams is not known, although it is likely that they are low-rank bituminous coals — that is, high volatile, bituminous C rank — which are typically in the low to moderately gassy range, as proposed by Thakur (2006). The dominant source of methane emissions to all deep longwall mines is the overlying and underlying coal beds within the zone of emissions, not the mined seam. The progressive sealing of the gob makes the tailgate corner an important location for methane emissions management. The tracer gas test findings have also demonstrated the interaction of face gas and GGVs.

Influence of barometric pressure

Diurnal variations in barometric pressure are pronounced at the study site due to the relatively high elevation, over 1,500 m (5,000 ft). Barometric pressure changes are shown each day of the study with time expressed on a 24-hour basis (Fig. 8). These diurnal variations shown are typical of the mine site with increases in daytime temperature beginning in the morning, usually between 9:00 and 10:00. Warm daytime air continues for the next 10 to 11 hours. The warmed air column produces a drop in atmospheric pressure during typical sunlight hours and allows the gas present in the sealed gob to expand. This produces emissions from the gob into active workings at the face and tailgate. Through the cooling evening and early morning hours, the denser air increases barometric pressure and promotes gas contraction within the gob. During this diurnal phase, the gases in the gob contract in response to increased barometric pressure, and emissions into active workings are expected to diminish. As previously noted, the mine operator avoids the migration of ventilation air leakage into the sealed gob through the addition of N_2 to make up for the volumetric loss of gob gas.

Figure 8 shows measurable diurnal changes in barometric pressure occurred during the field study. All plots are shown with daily data from midnight to midnight. The highest atmospheric pressure measured was on day 1, and later in the day the largest single-day pressure decrease was measured during the study. On day 2, the start of face emissions monitoring, daytime barometric pressures began at a relatively low level and experienced a relatively diminished drop, although the minimum pressure was the lowest level recorded. Day 4 produced the second highest daytime barometric pressures during the study. A change in barometric pressure over the course of day is measured from 00:01 to 24:00 midnight.

Table 3 gives a summary of face methane flows measured at the tailgate sensor, the 24-m (80-ft) sensor, GGV methane production from boreholes gas 4, 5 and 6. The gas produced by the GGVs was typically in excess of 95 percent methane (CH_4) and averaged below 1 percent oxygen (O_2). The underground data include only one set of mine operator data. The data do not show a general correspondence between the barometric pressure changes and methane flows measured underground or at the surface. No influences of barometric pressure fluctuation on the emissions from the face or at the 24-m (80-ft) sensor were observed. An exception may have occurred toward the end of the shift on day 4 where gas

flows at the 24-m (80-ft) sensor decreased when production on the face was active, possibly due to rising barometric pressure (Figs. 7 and 8).

A pattern of declining methane production from GGVs with increasing distance from the face was observed. This decline occurs relatively close to the longwall face, although at this close spacing it is expected that GGVs are essentially competing for gas from the same reservoir formed by the longwall gob (Schatzel, Krog et al., 2012).

The rate of N_2 injection was measured but the specific distribution of this gas underground among multiple distribution locations was not recorded. Within the limits of the data set, plots of N_2 flow and barometric pressure are shown for days 2 and 4 of the study. A general pattern of increasing pressure as part of the diurnal cycle occurs on both days from midnight until the morning hours of about 08:00 to 10:00 (Figs. 9 and 10). The N_2 injection rate remained relatively constant during this time on Day 2 and changed very little over the remainder of the day. On Day 4, the rate of N_2 injection initially declined then remained quite constant until the early evening when flow rates declined again. During the period of relatively constant N_2 flow, barometric pressure was declining until the afternoon when pressures rose again. The N_2 flow measured by the mine operator may correspond to the general pressure measured on Day 4. A similar correspondence was not observed on Day 2, partially because the rate of injection was quite consistent and there was decrease in barometric pressure over the same time frame. These observations make no assumption about the relative success of the strategy used by the mine operator to inject N_2 into portions of the sealed areas during periods of increasing barometric pressure.

Interactions between face ventilation air and longwall gobs

Tracer gas data from the study site show that a limited portion of the SF_6 from the face release reached operational gob gas ventholes. Although the quantity of tracer recovered from the GGVs was very small — approximately 0.3 percent — the activity of the exhauster on the borehole produced a localized low-pressure zone in the vicinity of the base of the borehole. Consequently, there is potential for the influence of face air movement toward the gob near the tailgate.

Mucho et al. (2000) had previously demonstrated that tracer gas released into an inactive, undermined GGV migrated through the fracture network to an adjacent, operating GGV. When the adjacent, operating GGV went off production, the tracer gas entered the ventilation system and eventually exited the mine from a bleeder fan. Although there are a range of GGV completion designs utilized by coal mine operators, data from the study by Mucho et al. (2000) show that gas being extracted by GGVs will enter the ventilation system if the borehole exhauster stops production. At the study site, the mine operator regularly utilizes the nearest operating GGV to manage face and tailgate corner methane concentrations.

Prior efforts by NIOSH and Australia’s Commonwealth Scientific and Industrial Research Organization (CSIRO) mining researchers have provided data and insights into permeability distributions in longwall gobs. Results published by Balusu, Tuffs and White (2006) showed a change in gob O_2 concentrations at an Australian longwall operation as a result of an

increase in face airflow rates and without any additional ventilation modifications, such as changes to the tailgate curtain or modifications to the distribution of air quantities at the tailgate corner. Karacan et al. (2007) performed novel numerical modeling methods and showed a permeability decrease of about two orders of magnitude within the mined coal horizon when moving from the edge to the center of the gob. Schatzel, Karacan et al. (2012) gave results on changing permeabilities over an active longwall panel where permeabilities reached at least 63 D in the overburden over the tailgate. Data also showed that maximum permeability in the gob overburden above the gateroads corresponded to maximum compaction above the panel centerline following undermining. Results from this study show the released tracer gas migrated from release point behind the face near the headgate with nearly simultaneous arrivals at shields 57 and 119, within one minute of each other. The bulk of the tracer gas slug, essentially indicated by the peak concentration, showed first at shield 119 before accumulating at shield 57. Consequently, this migration is thought to be evidence of more than one pathway of movement to these locations (Fig. 11). The decrease in permeability in the central portion of the gob both at the mining horizon and in the longwall panel overburden may be an important factor in producing this airflow pathway. A pathway for face air to move behind the face and into the gob must also exist to account for tracer gas production from GGVs 4, 5 and 6. A pathway is shown by the dotted line in Fig. 11, which has been drawn from behind the shields to the face air ventilation near shield 57.

Summary and conclusions

A study of face gas movement, methane movement and near-gob involvement was conducted using both tracer gas testing techniques and face emissions monitoring. Tracer gas testing, using a rapid release behind the first few headgate shields, recovered about 190 percent of the released SF_6 at the nearest monitoring point. The primary source of error in this calculation was concentration quantification for the samples most enriched in SF_6 using the analytical method. Airflow pathways exist in front of and behind the shield line from release point to the sample tubes. The data suggest that void space is present behind the shields. Migration rates of tracer gas, paralleling the gateroads near the panel margin and through the fractured gob overburden, are similar to what had been previously measured in the Northern Appalachian Basin in the mining of the Pittsburgh coalbed. Barometric pressure variations were monitored at the surface and showed a considerable range. A relationship between tailgate methane emissions and barometric pressure was not observed. However this study included only the daylight production shift such that the effects of diurnal barometric pressure variations may not be fully assessed in the data set.

Based on the findings from this study, a few suggestions were formulated to improve methane emissions management at the longwall face. The tracer gas data from this study demonstrate that airflow patterns on the longwall are likely more complex than simple linear flow paths. Ground movement characteristics are an important factor in determining the shape and volume of the void space that is created behind shields — that is, caving characteristics may produce a very large void, or roof rock breakage may fill much of this space once the shields advance. The findings from the tracer gas portion of this study showed that there was interaction between the three GGVs closest to the face — 30 to 170 m (100 to 570 ft) — and face ventilation airflow.

Methane levels showed little increase from the headgate to the tailgate corner, although production delays were occurring due to high methane concentrations. The near-face automated sampling instrumentation indicated the largest increases in methane concentrations and flow at the outby tailgate 24-m (80-ft) sensor. The data suggest that communication with the gob through the tailgate gateroad is the primary source of problematic emissions, with daily average methane concentrations increasing by no more than 0.1 percent from headgate to tailgate. Consequently, improved dilution of methane in face air may have a limited effect where the dominant source of methane emissions occurs from the gob of the active panel and migrates past the tailgate corner. Due to communication between the GGVs and the face ventilation, it may be possible to improve tailgate emission rates through improved GGV performance. Additional face airflow can provide increased methane dilution along the face and at the tailgate.

Data from the tracer gas field experiment imply that the movement of air at the face was influenced by void space and gob permeability distributions near the gateroads. From NIOSH's experience with SF_6 as a tracer gas, the movement of the tracer gas at low concentrations is identical to the movement of ventilation air once it is mixed in the airstream. Consequently, the movement of the tracer gas depicts ventilation air movement starting with the described release location. The movement of the tracer within or behind the shields and along the face, is shown to be generally from head to tail. In addition to moving outby from the tailgate corner, some ventilation flow moved inby toward the GGVs near the tail following the permeability distribution on a supercritical longwall.

The proposed distribution of face air has some important implications regarding the control of methane on longwall faces and in gobs. From the release location behind the longwall face, the tracer gas (and ventilation air) both stayed within the shields and moved onto the face. The ventilation air moved down the face toward the tail. At the tailgate corner a portion of the gas moved inby toward a GGV location and most moved outby. Data from this study suggest a correlation between patterns of face longwall face airflow and subsidence profiles in the gob. Ultimately, the caving and induced fracturing of overburden may be much more important to gas movement than overburden lithology or permeability as the strata break in accordance with engineering designs. However, the shallow, near-face gob certainly can produce either bridging or brittle breakage of rock units and may affect airflow patterns on longwall faces. The relatively open near-gob conditions at the study site may have played a role in dictating the observed face air flow patterns.

References

1. American Society of Testing Materials (ASTM). Standard Test Method for Volumetric and Mass Flow Rate Measurement in a Duct Using Tracer Gas Dilution. ASTM; 1999. E 2029-99
2. American Society of Testing Materials (ASTM). Standard Test Method for Determining Air Change in a Single Zone by Means of a Tracer Gas Dilution. ASTM; 2000. E 741-00
3. Balusu R, Tuffs N, White D. Surface goaf gas drainage strategies for highly gassy coal mines. Journal of the Mine Ventilation Society of South Africa. 2006; 59:77–84.
4. Diamond, WP., Jeran, PW., Trevits, MA. Evaluation of Alternative Placement of Longwall Gob Gas Ventholes for Optimum Performance. U.S. Department of the Interior, Bureau of Mines; 1994. p. 14Report of Investigations 9500, NTIS No. PB 94-171949

5. Grot RA, Lagus PL. Evaluation of ventilation systems using tracer gas methods. Industrial Hygiene News. 1991; 14(6)
6. Hartman, HL., Mutmansky, JM., Ramani, RV., Wang, YJ. Mine Ventilation and Air Conditioning. 3. Wiley; New York: 1997. p. 729
7. Karacan CÖ. Modeling and prediction of ventilation methane emissions of US longwall mines using supervised artificial neural networks. International Journal of Coal Geology. 2008; 73:371–387. https://doi.org/10.1016/j.coal.2007.09.003.
8. Karacan CÖ, Esterhuizen GS, Schatzel SJ, Diamond WP. Reservoir Simulation-Based Modeling for Characterizing Longwall Methane Emissions and Gob Gas Venthole Production. International Journal of Coal Geology. 2007; 71:225–245. https://doi.org/10.1016/j.coal.2006.08.003.
9. Krog, RB., Schatzel, SJ., Garcia, F., Marshall, JK. Predicting methane emissions from longer longwall faces by analysis of emission contributors. In: Mutmansky, JM., Ramani, RV., editors. Proceedings of the 11th U.S./North American Mine Ventilation Symposium. Balkema Publishers; 2006. p. 383-392.
10. Mucho, TP., Diamond, WP., Garcia, F., Byars, JD., Cario, SL. Implications of recent NIOSH tracer gas studies on bleeder and gob gas ventilation design; SME Annual Conference & Expo; Feb. 28-Mar. 1, 2000; Salt Lake City, UT. Englewood, CO: Society for Mining, Metallurgy & Exploration; 2000.
11. National Institute for Occupational Safety and Health (NIOSH). Sulfur hexafluoride by portable GC, NIOSH method 6602. NIOSH Manual of Analytical Methods, 2003-154, 3rd supplement. 1994. https://www.cdc.gov/niosh/docs/2003-154/method-i.html
12. Palchik V. Formation of fractured zones in overburden due to longwall mining. Environmental Geology. 2003; 44:28–38.
13. Schatzel, SJ., Diamond, WP., Garcia, F., LaScola, JC., McCall, FE., Jeran, PW., Mucho, TP. An investigation of longwall gob gas behavior and control methods. In: Tien, J., editor. Proceedings of the 8th U.S. Mine Ventilation Symposium. Rolla, MO: 1999. p. 43-51.
14. Schatzel, SJ., Krog, RB., Garcia, F., Marshall, JK., Trackemas, J. Prediction of longwall methane emissions and the associated consequences of increasing longwall face lengths: a case study in the Pittsburgh coalbed. In: Mutmansky, JM., Ramani, RV., editors. Proceedings of the 11th U.S./North American Mine Ventilation Symposium. Balkema Publishers; 2006. p. 375-382.
15. Schatzel SJ, Karacan CÖ, Dougherty H, Goodman GVR. An analysis of reservoir conditions and responses in longwall panel overburden during mining and its effect on gob gas well performance. Engineering Geology. 2012; 127:65–74. https://doi.org/10.1016/j.enggeo.2012.01.002.
16. Schatzel, SJ., Krog, RB., Dougherty, H. Methane emissions and airflow patterns on a longwall face; SME Annual Conference & Expo; Feb. 19–22, 2012; Seattle, WA. Englewood, CO: Society for Mining, Metallurgy & Exploration; 2012. p. 72-78.Preprint 12-016
17. Schmidt D. The benefits of degasification. Coal Age. 2016; 14(3):28–30.
18. Singh, MM., Kendorski, FS. 1st Conference on Ground Control in Mining. Morgantown, WV: 1981. Strata disturbance prediction for mining beneath surface water and waste impoundments; p. 76-89.
19. Srinivasa, Rao, BM., Baafi, EY., Aziz, NI., Singh, RN. Proceedings of the Sixth US Mine Ventilation Symposium. Society for Mining, Metallurgy & Exploration; Englewood, CO: 1993. Three dimensional numerical modelling of air velocities and dust control techniques in a longwall face.
20. Thakur, PC. Chapter 6—Coal Seam Degasification. In: Kissell, F., editor. Methane Control Handbook. U.S. Department of Health and Human Services; 2006. p. 77-96.IC 9486
21. Thimons, ED., Kissell, FN. Tracer Gas as an Aid in Mine Ventilation Analysis. U.S. Department of the Interior, Bureau of Mines; 1974. p. 17Report of Investigations, No. 7917, NTIS No. PB234051

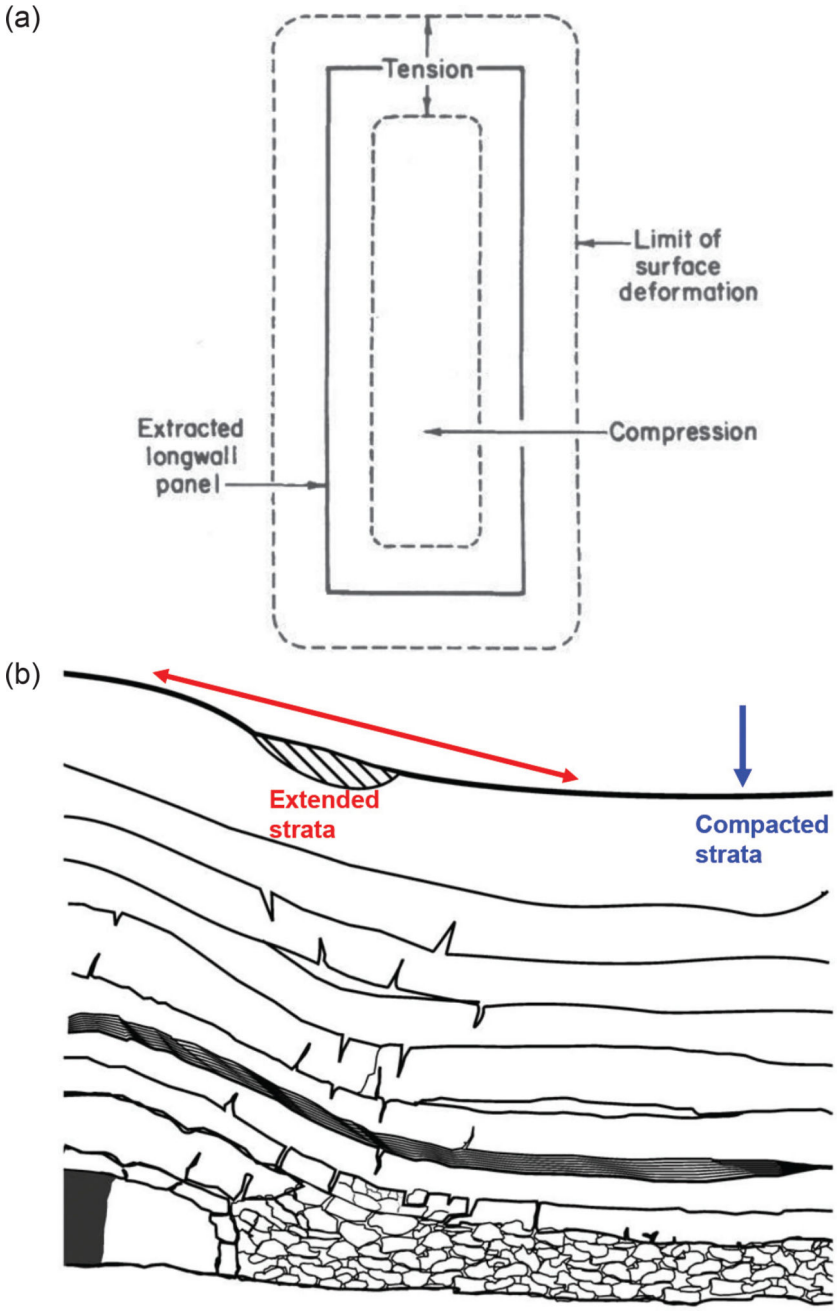

Figure 1.

(a) A hypothetical cross-section (not to scale) of a longwall panel gob viewed parallel to the face and extending from the panel margin to the panel centerline. Compaction of strata after removal of the mined seam near the panel centerline extends the overburden at locations near the longwall panel margin (Schatzel et al., 2012). (b) Map view of a generalized distribution of overburden rock stresses above a longwall gob. Tensional zone exists following the outline of the panel both on the inside and outside at the surface above the panel. Moving from the panel outline toward the centerline, tensional rock stress decreases

in magnitude and transitions to compressional stress (Diamond, Jeran and Trevits, 1994; Schatzel et al., 2012).

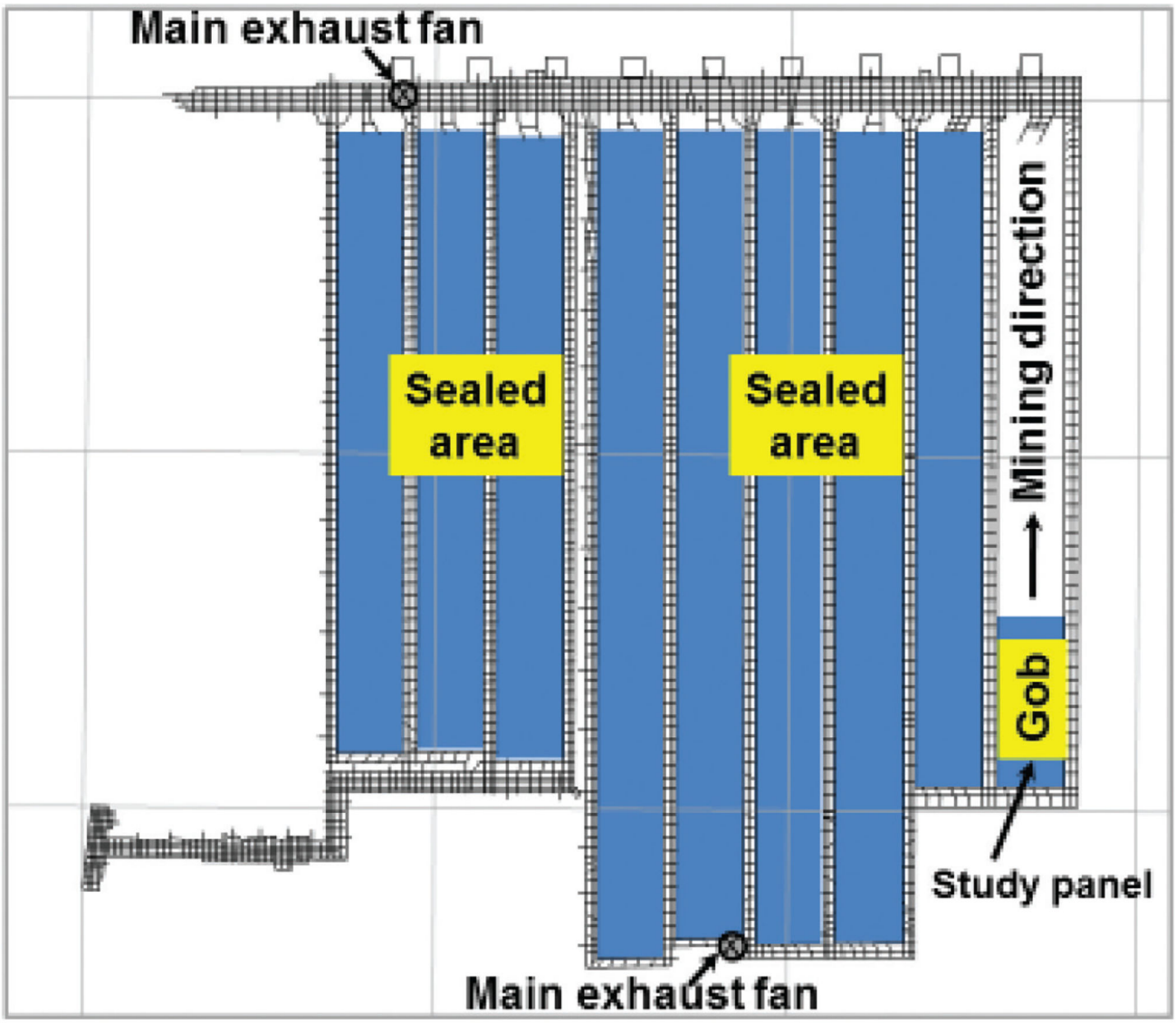

Figure 2.
Site map including the multiple panel section, surface fans and study panel.

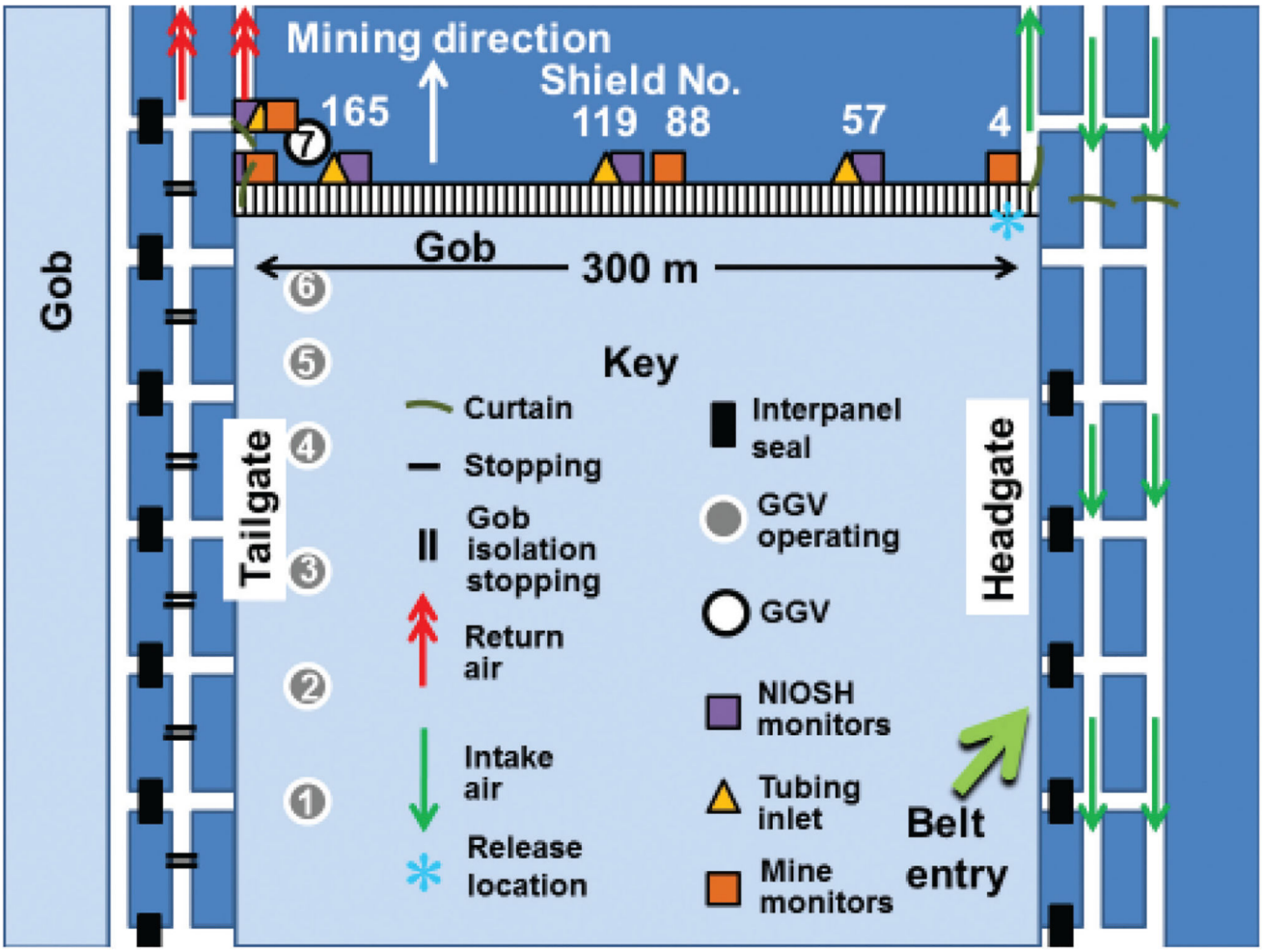

Figure 3.

Study site ventilation and instrumentation for monitoring SF_6 flow and methane emissions. Entry numbering is from right to left on both the headgate and tailgate gateroads in the orientation shown.

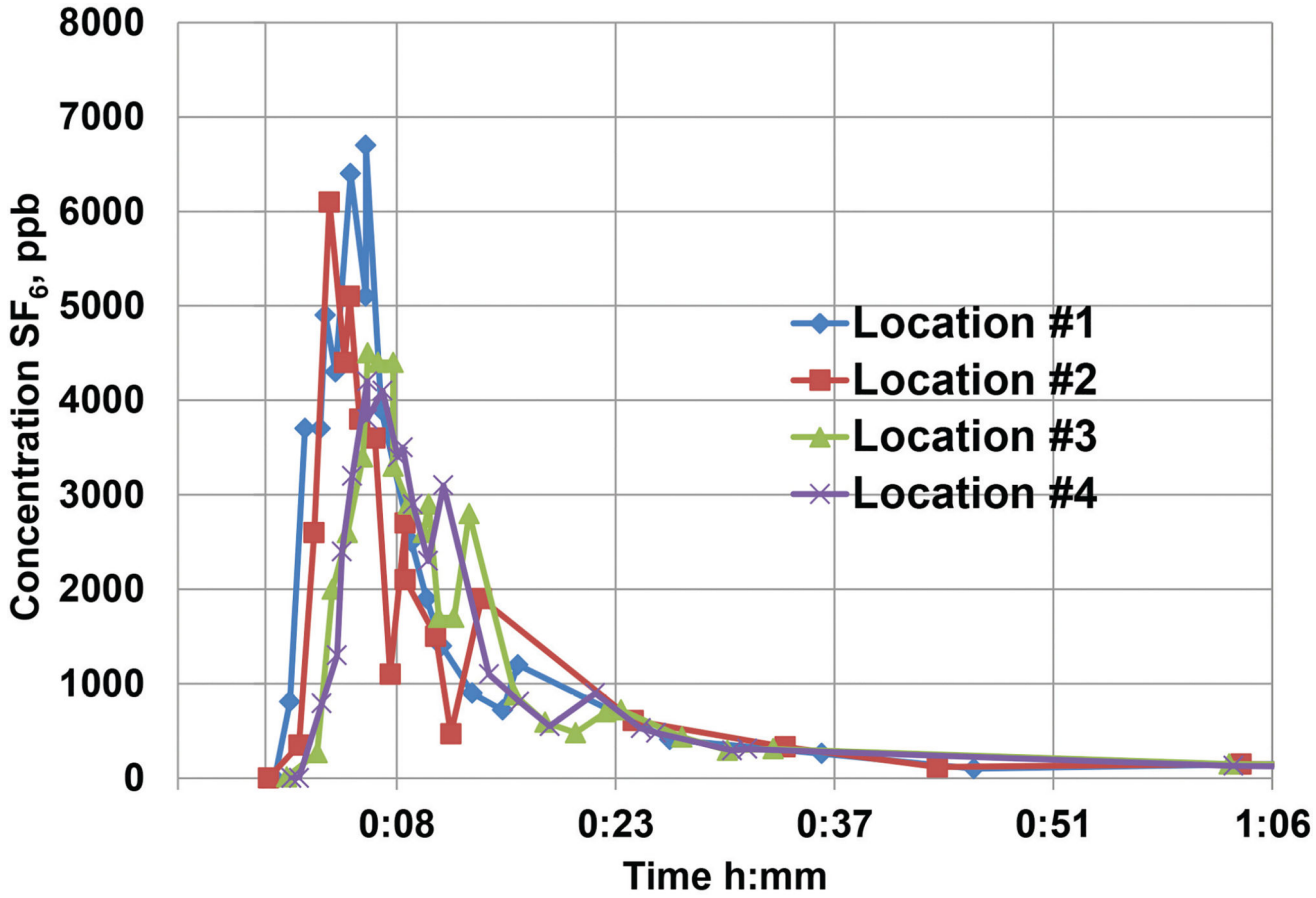

Figure 4.
Corrected tracer gas accumulations at underground near-face locations. Location 1 is shield 57, location 2 is shield 119, location 3 is shield 165 and location 4 is the 24-m (80-ft) sensor position.

Figure 5.
Gas sampling at an active gob gas venthole (GGV).

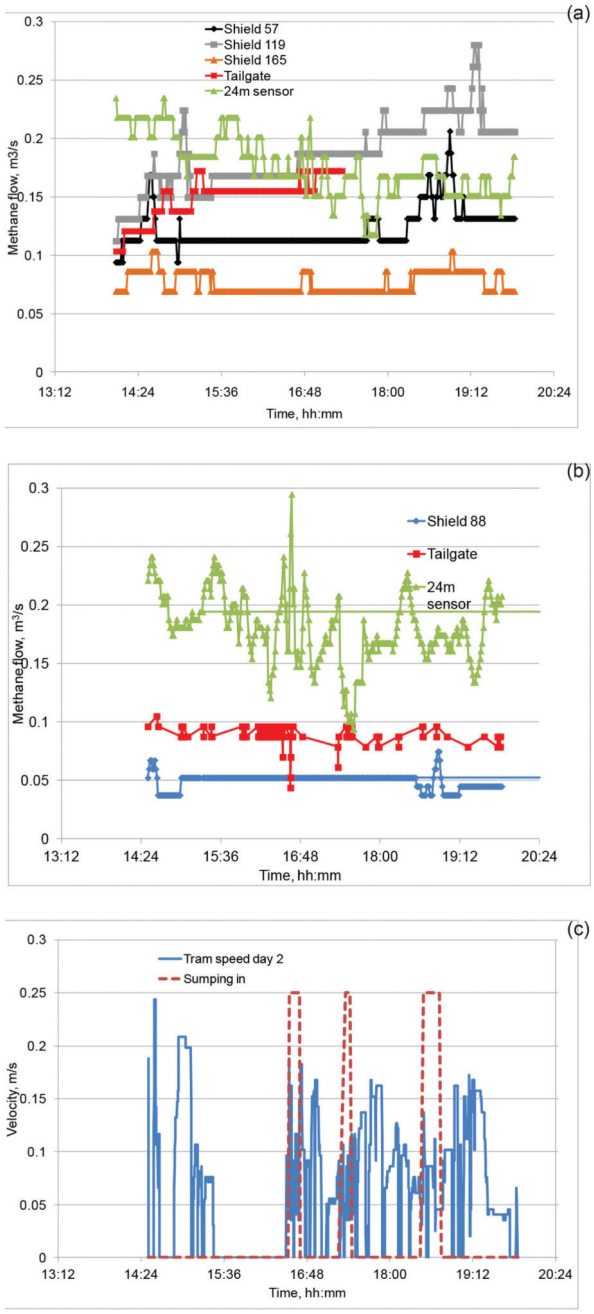

Figure 6.

Day 2 face emissions: (a) NIOSH instruments, (b) mine operator instruments and (c) shearer tram speed and sumping activity.

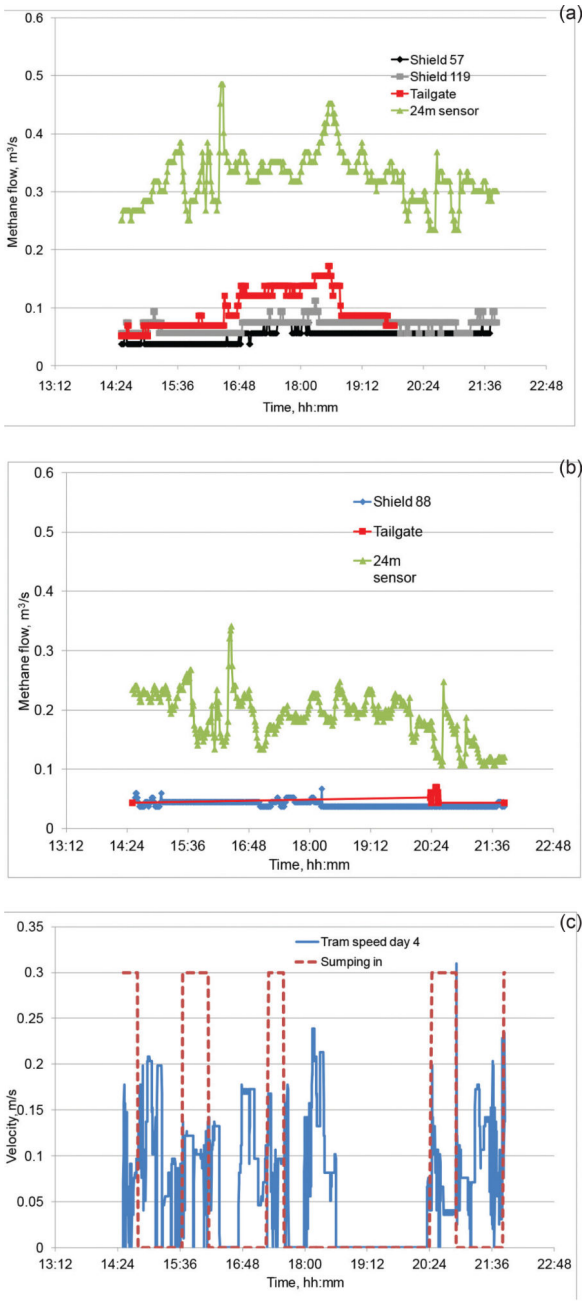

Figure 7.

Day 4 face emissions: (a) NIOSH instruments, (b) mine operator instruments and (c) shearer tram speed and sumping activity.

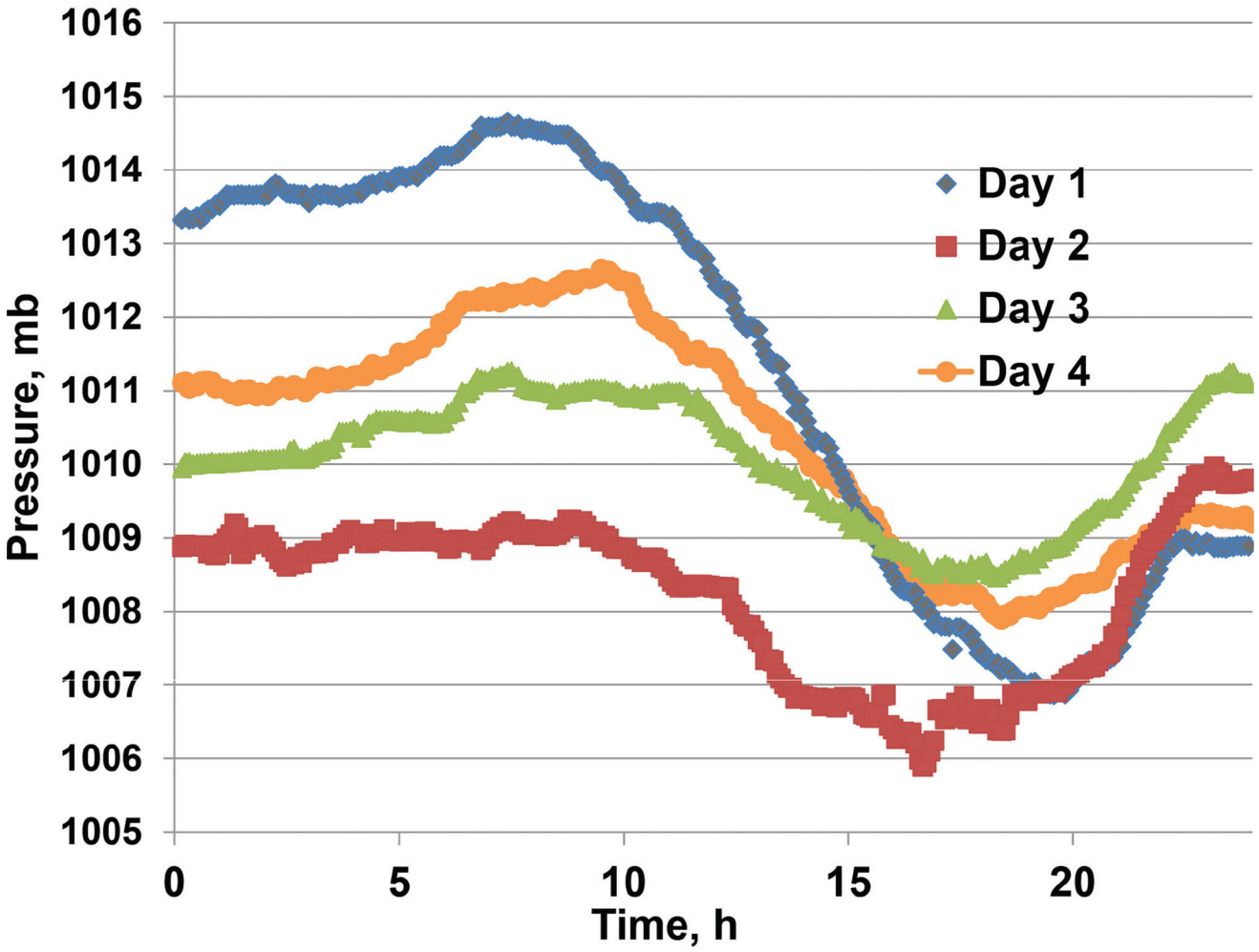

Figure 8.
Barometric pressure variations over the duration of field testing corrected to sea-level pressure.

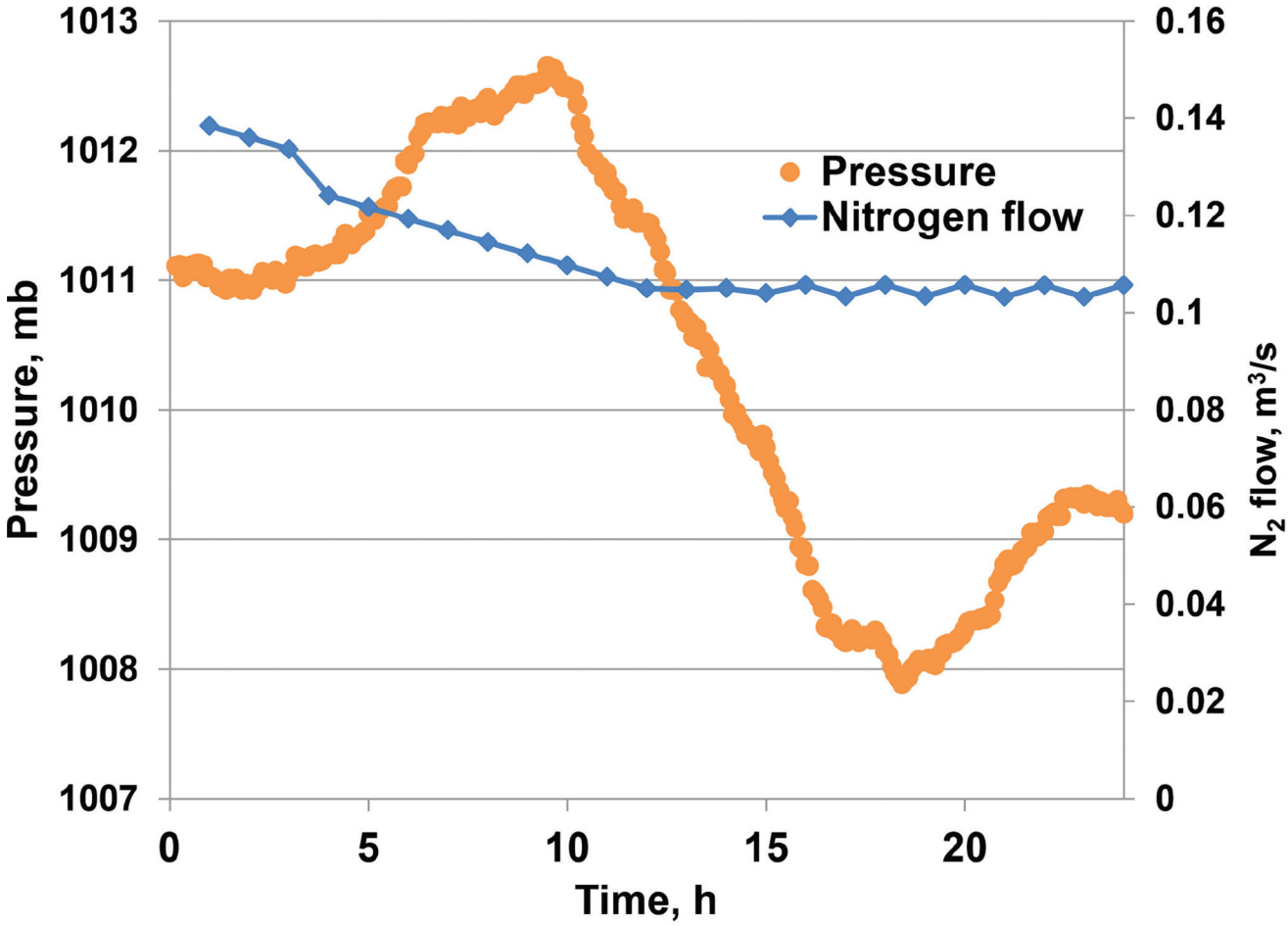

Figure 9.

Correspondence between rate of nitrogen injection at longwall panel headgate and barometric pressure, Day 2. Monitoring systems are programmed to record changes in conditions in flow or pressure conditions.

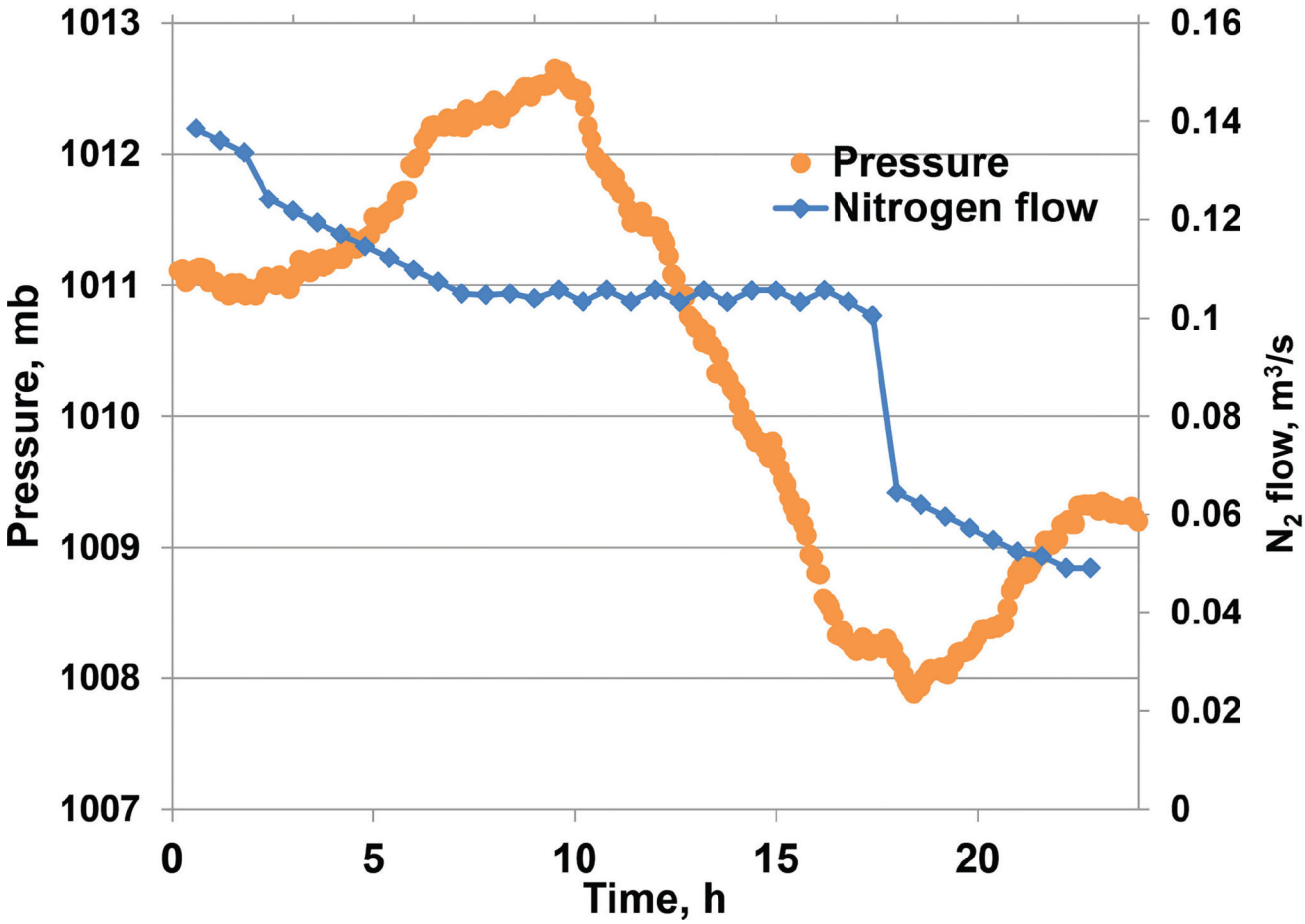

Figure 10.

Correspondence between rate of nitrogen injection at longwall panel headgate and barometric pressure, Day 4. Monitoring systems are programmed to record changes in conditions in flow or pressure conditions.

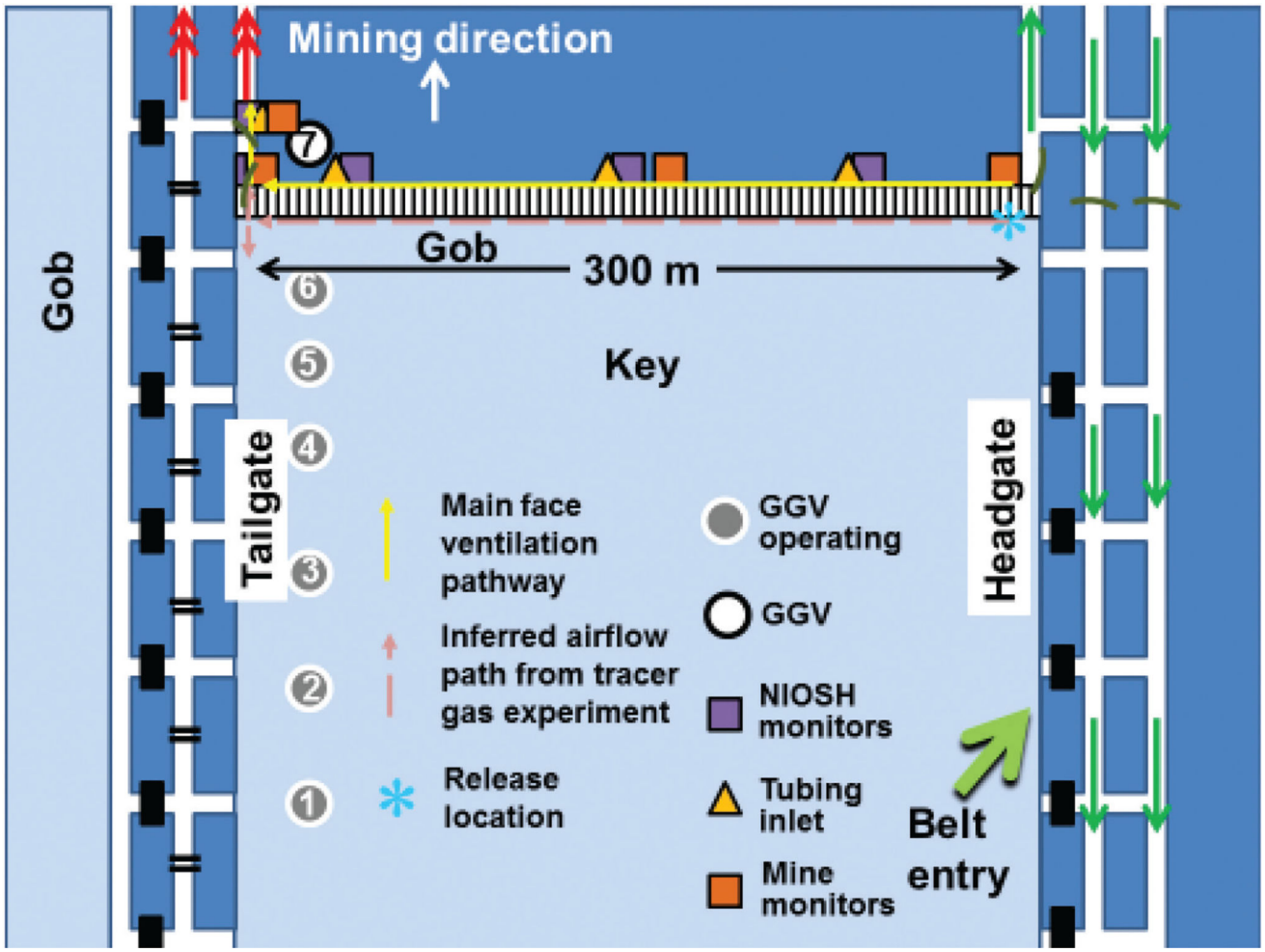

Figure 11.
Proposed airflow paths on longwall face at study site.

Table 1

Ventilation air and tracer gas transit parameters along longwall face.

Location	Shield no.	Distance (m / ft)	Transport elapsed time, measured (s)	Velocity, measured (m/s / ft/min)	Velocity, SF_6 arrivals (m/s / ft/min)	Velocity, SF_6 peaks (m/s / ft/min)
1	57	96.4 / 316	32	3.03 / 596	1.66 / 326	0.35/ 68
2	119	205 / 673	68	3.02 / 595	1.74 / 342	1.24 / 245
3	165	286 / 939	130	2.2 / 433	1.61 / 316	1.01 / 198
4	24-m (80-ft) sensor	355 / 1,165	148	2.4 / 473	1.99 / 392	1.25 / 245

Table 2

Gob gas venthole production, tailgate concentrations and barometric pressure summaries (ND = not detected).

	Average CH_4 production (m^3/s / cfm)			Tailgate CH_4 flow	24-m (80-ft) sensor	Surface barometric pressure change (mbar)		
	GGV borehole 6	GGV borehole 5	GGV borehole 4			Minimum	Maximum	Change
Day 1	355	261	190	ND	ND	1,006.86	1,014.65	−7.79
Day 2	353	260	141	187	382	1,005.89	1,009.96	−4.07
Day 3	334	239	141	ND	ND	1,008.46	1,011.26	−2.80
Day 4	346	240	125	100	397	1,007.88	1,012.65	−4.77

Table 3

Longwall face methane emission daily averages.

Mine operator instruments	CH_4 flow (m^3/s / cfm)		
	Average	Minimum	Maximum
Study day 2			
Headgate	0.0374 / 79.2	0.0374 / 79.2	0.0374 / 79.2
Shield 88	0.0496 / 105	0.0373 / 79.0	0.0746 / 158
Tailgate	0.0883 / 187	0.0436 / 92.4	0.105 / 222
24-m (80-ft) sensor	0.180 / 382	0.0939 / 199	0.295 / 625
Study day 4			
Headgate	0.0374 / 79.2	0.0374 / 79.2	0.0374 / 79.2
Shield 88	0.0411 / 87.1	0.0373 / 79.0	0.0670 / 142
Tailgate	0.0472 / 100	0.0436 / 92.4	0.0698 / 148
24-m (80-ft) sensor	0.187 / 397	0.107 / 227	0.342 / 724